Copper–Metallomesogen Structures Obtained by Ionic Self-Assembly (ISA): Molecular Electromechanical Switching Driven by Cooperativity

Franck Camerel,[a] Peter Strauch,[b] Markus Antonietti,[a] and Charl F. J. Faul*[a]

Abstract: In a stepwise noncovalent multiple-interaction strategy, copper(II) salts were complexed with the sodium salts of bathophenanthrolinedisulfonic acid (BPS) and bathocuproinedisulfonic acid (BCS), and organized into nanostructured materials by the addition of ammonium surfactants by means of the ionic self-assembly (ISA) route. In the case of the methyl-substituted BCS complexes, a slow color change from green to brick red was observed. UV and EPR investigations showed that the color change was due to a change in oxidation state, the resulting brick red color is typical for Cu^{I} species. It is concluded that steric interactions and mechanical packing into a supramolecular structure drive this electronic transition at the metal center. When complexation is performed with double-tail ammonium surfactants, these metallomesogenic materials exhibit thermotropic liquid-crystalline phase behavior, as investigated by polarized light microscopy, differential scanning calorimetry (DSC), and temperature-dependent wide-angle and small-angle X-ray analyses. The complexity of the observed phases increased with increasing tail length of the surfactants. Complexation with double-tail C_{18} surfactants yielded highly organized materials for both the BPS and BCS ligands.

Keywords: coordination chemistry · ionic self-assembly · nanostructures · supramolecular chemistry · surfactants

Introduction

Metal coordination[1] is one of the key design principles in supramolecular chemistry.[2] Related to this, considerable research effort has also been invested to organize metal-containing species into soft liquid-crystalline materials (metallomesogens) that combine the unique properties of the anisotropic fluids (e.g. fast orientational response to external fields) with the specific properties of metals (e.g. magnetic and electronic properties).[3] Liquid crystals incorporating paramagnetic metal ions (such as Cu^{II}) are of particular interest because they can be switched by weak external magnetic fields and are finding new applications in display and communication technologies.[4]

Phenanthroline and its derivatives are powerful tectons for this purpose, and lyotropic and thermotropic liquid-crystalline materials based on these chelating agents have been described.[5] The chemical and physical properties of coordination complexes of 1,10-phenanthroline derivatives (with two

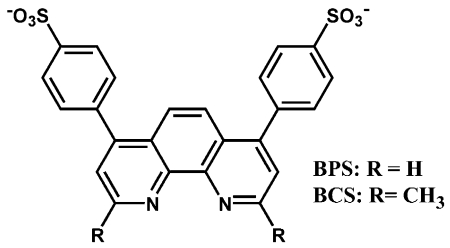

sulfonate groups on the phenyl groups in the 4,7 positions of the phenanthroline, making the ligand water soluble) have been widely studied and used for separation of metallic atoms such as Fe^{II}, Ni^{II}, Co^{II}, Cu^{II}, Zn^{II} by chromatography or capillary electrophoresis,[6, 7] as well as for the development of bio-inorganic probes.[8] Furthermore, the presence of methyl groups in the 2,9 positions of the phenanthroline is known to influence the coordination geometry around the copper center. For example, Cu^{II} complexes with nonsulfonated parent ligands are usually fivefold coordinated. The structure of $[Cu^{II}(phen)_2(H_2O)]^{2+}$ is less distorted (with a dihedral angle between the two planes of ca. 30°) than the bis(2,9-dimethyl-1,10-phenanthroline)copper(II) analogue $[Cu(dmp)_2(H_2O)]^{2+}$ (with a dihedral angle of ca. 70° and much closer to a tetrahedral complex).[9] This provides the possibility to change or influence the self-assembly architecture, and therefore also the physical properties (electronic, optical and material properties) of the liquid-crystalline complex phases.

[a] Dr. C. F. J. Faul, Dr. F. Camerel, Prof. Dr. M. Antonietti
Max Planck Institute of Colloids and Interfaces
Research Campus Golm, 14424 Potsdam-Golm (Germany)
Fax: (+49) 331 567 9502
E-mail: Charl.Faul@mpikg-golm.mpg.de

[b] Prof. Dr. P. Strauch
Institute of Chemistry
University of Potsdam, 14415 Potsdam (Germany)

DOI: 10.1002/chem.200204693

It was recently reported[10] that the inorganic crown species $[Ni_3S_3P_{12}]^{3-}$ could be organized into soft materials by the process of ionic self-assembly (ISA).[11] These complexes showed, due to their special supramolecular order, rather unexpected solid–solid transitions.[10] This route therefore provides the possibility to not only tune the phase behavior, but also the chemical response of such soft matter complexes.

ISA is a technique that organizes charged organic oligoelectrolytic species (such as dyes), by oppositely charged counterions with complementary properties (e.g. surfactants).[11] The hierarchical superstructure is then controlled by secondary interactions, such as hydrophobic segregation or $\pi-\pi$ interactions of the conjugated flat molecules, as is now well known for discotic liquid-crystalline phases.[12]

The aim of this investigation is to organize metal ions by ISA of the corresponding phenanthroline complexes, and to find new pathways to tune not only their phase behavior, but also their chemical and physical response. As an extension of the above-mentioned principles, a multiple-interaction strategy is applied in which water-soluble chelating agents with a charged group in the periphery (disodium bathophenanthrolinedisulfonate (BPS) and disodium bathocuproinedisulfonate (BCS)) are utilized. After chelation of copper(II) salts, the resulting complexes are employed as tectonic units in an ISA process and assembled with a variety of surfactants (Scheme 1). The ability of the resulting bulk materials to undergo physical phase changes as well as chemical changes is then investigated in detail.

This process for the construction of liquid-crystalline materials (based on stepwise noncovalent interactions) allows easy tuning of the properties of the resulting structures by careful choice of the metal, the ligand, and the alkyl volume fraction ('internal solvent') by simple exchange of the binding partner in the respective assembly step without tedious synthetic operations.

Results and Discussion

Copper complexes are obtained at room temperature in water by direct addition of two equivalents of the BPS and BCS ligands to an aqueous solution of $CuCl_2$.[13] A light-green complex is obtained in the case of the BPS ligand and an olive-green complex in the case of the BCS ligand. These complexing agents reacted in a similar way as their non-phenylsulfonated parent molecules 1,10-phenanthroline (phen) and 2,9-dimethyl-1,10-phenanthroline (dmp).[6] Both copper complexes (in the solid state and in aqueous solution) are five-coordinate; the copper center displays a distorded trigonal-bipyramidal geometry, and is surrounded by a chloride ion and four N atoms from two phenathroline species.[14]

After addition of the oppositely charged surfactants, a colored precipitate is obtained (except for the case of the $CuCl_2$/BCS/C_{16}TA complex where no precipitation was found). The precipitated products from the BPS ligand were green, as expected for Cu^{II} complexes. However, precipitates from the BCS ligand turned dark red after several hours of stirring at room temperature. Control experiments, without the addition of surfactants, showed that the BCS complexes only turned red after several months at room temperature or alternatively, turned red after boiling for about 2 h. 2,9-Methyl-substituted phenanthrolines are known to give red complexes with Cu^{I}.[14, 15] This red color is attributed to an intense metal-to-ligand charge-transfer (MLCT) band in the four-coordinate tetrahedral Cu^{I} complexes[16] (dihedral angle close to 90°). This is observed in the range 450–480 nm and proved to be useful in colorimetric analysis schemes.[14, 15, 17]

The copper–phenanthroline derivative surfactant complexes were characterized by UV/Vis spectroscopy (Figure 1). Both the free ligand and the metal chelates give strong absorption in the ultraviolet region between 250–300 nm due to the conjugated structure of the phenanthroline derivatives, that is, intra-ligand $\pi-\pi^*$ absorption.[7, 18] The absorption maxima (λ_{max}) of BPS and BCS chelates, at 285 and 288 nm respectively, show a small blue shift compared to the maxima of the free ligands BPS and BCS (278 and 285 nm), indicative of the coordination of the copper ion by the ligand. The electronic absorption spectra of the green BPS complexes in solution and in the solid state, show single, very broad, d–d bands in the visible region with a maximum at about 730 nm, which tail to 800 nm, consistent with five-coordinate distorted trigonal-bipyramidal Cu^{II} complexes.[19] The absorption band (observed at 479 nm in the case of the BCS chelates) in the visible region corresponds to the metal-to-ligand charge-transfer ($d-\pi^*$) absorption, which is characteristic of tetrahedral Cu^{I} complexes with a CuN_4 coordination sphere and a dihedral angle close to 90°.[20]

The formation of the red copper(I) complex $[Cu(BCS)_2]^{3-}$ from the original complex $[Cu^{II}(BCS)_2(Cl)]^{3-}$ upon addition of surfactants is also confirmed by EPR spectroscopy. A broad

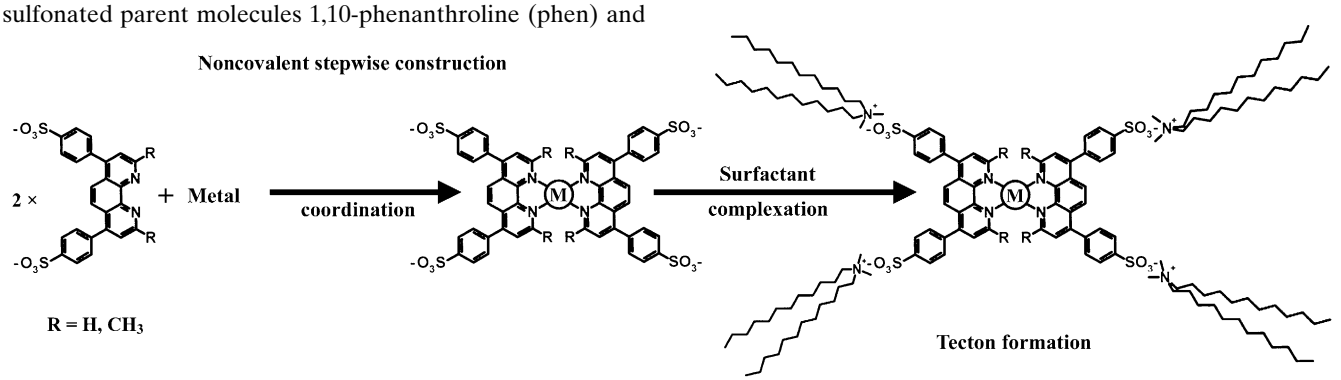

Scheme 1. Construction of the tectons used for the production of liquid-crystalline materials based on stepwise noncovalent interactions.

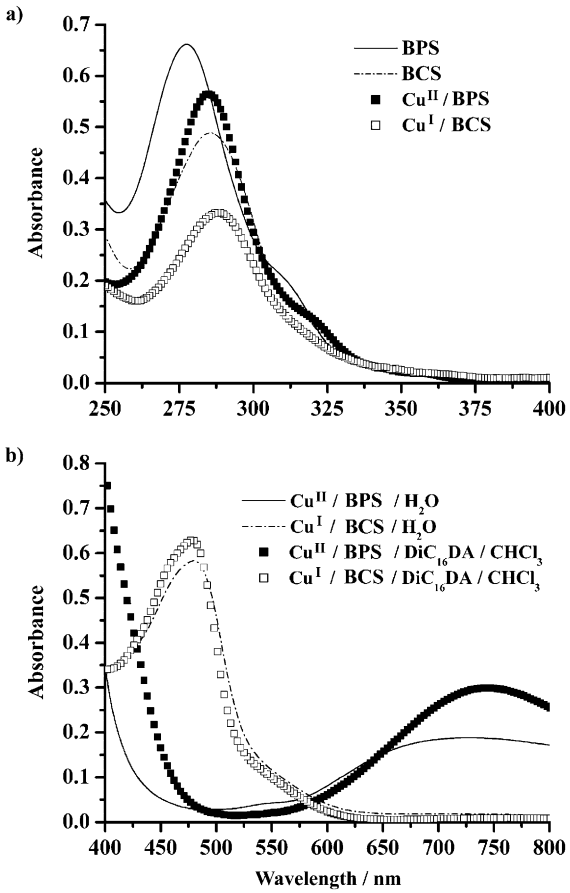

Figure 1. UV/Vis spectra of the pure chelating agents and of the corresponding copper complexes. a) Ultraviolet region (250–400 nm) ($c = 1.56 \times 10^{-5}$ mol L^{-1}); b) visible region (400–800 nm) (for BPS complexes $c = 2.0 \times 10^{-3}$ mol L^{-1} and for BCS complexes $c = 2.5 \times 10^{-4}$ mol L^{-1}).

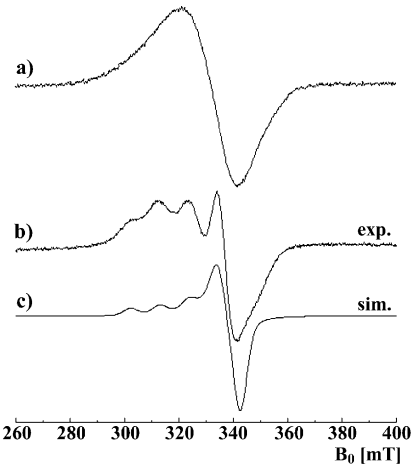

Figure 2. EPR studies of the complex $CuCl_2$/BPS/DiC_{16}DAB in solution and in the solid state: a) EPR spectrum of the copper(II) complex in the solid state at room temperature; b) EPR spectrum of a solution of the copper(II) complex in $CHCl_3$; and c) a simulation of the axially symmetric spectrum .

unresolved line at 330 mT ($g = 2.1$) can be observed for the green paramagnetic copper(II) complex $[Cu^{II}(BPS)_2(Cl)]^{3-}$. The red copper(I) complex is EPR-silent or only traces of paramagnetism can be detected. The very broad line (ca. 70 mT) at 330 mT is due to copper–copper interactions in the nondiluted system and does not permit further interpretation (Figure 2a). Interestingly, the solutions of the green copper(II) complex in $CHCl_3$ do not give the expected isotropic spectrum of a diluted monomer. The solution spectrum is still anisotropic with axial symmetry, superimposed by a broad line of undefined paramagnetism, indicating a high level of association in solution as well. Figure 2b shows the spectrum of the copper(II) complex in solution, and a simulation of an anisotropic spectrum with the parameters $g_{\parallel} = 2.195^{\pm 0.005}$, $g_{\perp} = 2.065^{\pm 0.005}$, and $A_{\parallel} = 110^{\pm 5}$, $A_{\perp} = 15^{\pm 5} \times 10^{-4}$ cm^{-1} is presented in Figure 2c.

Evidently, addition of surfactant to the BCS chelates and the resulting cooperative structure formation lead to the conversion of Cu^{II} to Cu^{I}, finally ending in a four-coordinate tetrahedral structure in which the ligands lie in approximately orthogonal planes (dihedral angle close to 90°). The presence of methyl groups close to the coordination sites on the BCS chelating agent force the system to adopt a tetrahedral structure. This coordination geometry is known to have a stabilizing effect on the copper(I) oxidation state. The reduction of the copper(II) to copper(I), as evidenced by the color change, is dramatically enhanced by addition of surfactant. This implies the removal of the chloride ion from the coordination sphere and the reduction of the copper species. It should be noted that the pH of the solution decreases during the formation of this copper(I) complex in water. Similar color changes were observed when similar investigations were performed with copper(II) with both bromide and the weaker-coordinating acetate counterions. It should also be noted that the presence of surfactant tails renders the copper(I) state stable in air.

We conclude that the reduction of the copper center is driven by a mechanism based on steric packing, exerted by the surfactant tails, that is the energy gain due to an optimized packing pattern changes the electrochemical potential of the metal complex. In other words: mechanical packing into a supramolecular structure drives an electronic transition in the inner center, that is an electromechanical coupling is observed due to the formation of an extended hybrid organic–inorganic moiety, which is already present in solution.

It appears that the BPS complexes that contain a Cu^{II} center in a distorted trigonal-bipyramidal geometry are stable even after surfactant complexation. This sensitivity of the molecular electromechanical switching against substitution indicates interesting geometrical/packing-induced influences on both the materials properties and their phase behavior.

The $(Cu^{II}–BPS)$–surfactant and $(Cu^{I}–BCS)$–surfactant complexes can be isolated, redissolved in chloroform, and cast into well-organized, dark but transparent films of sufficient mechanical quality. This allows the structural characterization of the long-range ordered state. Elemental analysis and ICP analysis show that the composition of the complexes is $[Cu^{II}(BPS)_2(Cl)] \cdot (Cl) \cdot (surfactant)_4$ and $[Cu^{I}(BCS)_2] \cdot (Cl) \cdot (surfactant)_4$ in the case of the double-tailed surfactants. In the case of the short single-tailed surfactants, for example C_{10}TA, the borderline case between simple counterion and surfactant is approached. This effect was already described for

dye – surfactant complexes, and leads to nonstoichiometric charge-ratio complexes.[11b] For the C_{16}TA complexes with BCS (which can only be extracted), an N:S ratio of 3.0:1 is observed. This indicates a ratio of two surfactant molecules per sulfonate charged group and will give rise to phase separation (as observed at high temperature in the solid state).

For the structural characterization, we included a wider variation of the cationic surfactant, and covered the range of alkyl tail lengths from 10 carbon atoms (1.4 nm, single tail) to 18 carbon atoms (2.4 nm, double tail). Table 1 provides an overview of the explored variety of structural elements in the formation of well-defined metal-chelate – surfactant complexes. All the complexes were characterized by differential scanning calorimetry (DSC), polarized optical microscopy (POM), temperature-dependent wide-angle and small-angle X-ray scattering (WAXS and SAXS). From TGA analyses the degradation temperature, in general, was found to be above 200 °C.

Single-tail surfactant complexes: In the case of the shortest surfactant tails (i.e., C_{10}TA, C_{12}TA), precipitation is observed, but only birefringent powders are obtained (see discussion on elemental analysis and stoichiometry above). DSC measurements show no transitions, and a broad peak can be detected on the SAXS curve which is attributed to a mean distance between the complexes larger than 3 nm. For the C_{10}TA/BPS complex, some additional reflections are observed but these could not be indexed to any known phase. No sharp reflections were detected in the WAXS region, and only a "sharp" halo has been detected, indicative of a semicrystalline arrangement of the side chains. Evidently, in these cases the volume fraction of alkyl tails is not high enough to support sufficient plasticity and packing.

For C_{16}TA complexes the geometry around the copper center starts to influence the packing properties. Films are formed that are birefringent under crossed polarizers. With BPS, a soft material is obtained, and no transition can be detected on the DSC curve. SAXS patterns display two broad peaks that can be indexed in a low-ordered lamellar system ($d_o = 4.19$ nm). Wide-angle X-ray scattering confirms that this material is "essentially" liquid-crystalline in nature with a broad halo in the WAXS region centered at 20° in 2θ. Temperature-dependent investigations confirmed the absence of structural changes in this material.

For the BCS complex with C_{16}TA a well-defined reversible transition is found at 101.2 °C. Temperature-dependent light microscopy investigations show a phase separation into an isotropic liquid and some small, unmelted crystallites at high temperature (above 120 °C). These crystallites probably consist of noncomplexed pure surfactants, based on the nonstriochiometric complexation detected by elemental analysis. Upon cooling the sample down to room temperature, we observed a fan-shaped texture typical for smectic B phases originating from the isotropic liquid (Figure 3). X-ray analyses confirm the presence of a smectic B phase structure after cooling from this mixed-phase state, but the origin of this phase cannot be unequivocally proven to arise from the formed copper complex.

These results from the two C_{16}TA complexes are indicative of the driving force of the originally found electronic transition ($Cu^{I} \rightarrow Cu^{II}$): instead of a low-ordered noncrystalline lamellar phase as found for BPS – Cu^{II}, a crystalline smectic B type arrangement is observed for BCS – Cu^{I}. This energetically favorable state of organization that exists for the BCS complex clearly provides the driving force for the change in oxidation state.

Double-tail surfactant complexes: For the double-tailed surfactants, the increase in the hydrophobic volume fraction makes the alkyl subphase the predominant phase, leading to softer or liquid-like materials (see Table 1).[11b] WAXS

Table 1. Overview of the investigated samples, their thermal behavior, and properties.

	BPS			BCS		
Surfactant	DSC	WAXS/POM	SAXS	DSC	WAXS/POM	SAXS
C_{10}TA	no transition	crystalline	phase not identified	no transition	crystalline	1 broad peak ($d = 3.12$ nm)
C_{12}TA	no transition	crystalline	1 broad peak ($d = 3.70$ nm)	no transition	crystalline	1 broad peak ($d = 3.25$ nm)
C_{16}TA	no transition	soft material	broad lamellar phase ($d_0 = 4.14$ nm)	1 reversible transition (101.2 °C)	crystalline	crystalline smectic B type phase ($a = 4.45$ nm and $d_o = 2.60$ nm)
$DiC_{10}DA$	no transition	soft material	1 broad peak ($d = 2.67$ nm)	no transition	gel	1 broad peak ($d = 2.44$ nm)
$DiC_{12}DA$	no transition	soft material	1 broad peak ($d = 2.87$ nm)	no transition	gel	1 broad peak ($d = 2.72$ nm)
$DiC_{14}DA$	no transition	soft material	1 broad peak ($d = 3.43$ nm)	no transition	gel	1 broad peak ($d = 3.22$ nm)
$DiC_{16}DA$	1 broad reversible transition (−20 °C)	soft material	lamellar phase ($d_0 = 3.95$ nm)	1 broad reversible transition (−19 °C)	soft material	nonindexed phase
$DiC_{18}DA$	3 transitions on the heating curve (23.6, 63.9, 113.1 °C) and 2 transitions on the cooling curve (102.7, 11.1 °C)	soft material	2 Columnar phases ((60 °C cooling): $a = 104.24$, $b = 60.58$ Å, $\gamma = 123°$; (45 °C heating): $a = 100.63$, $b = 58.57$ Å, $\gamma = 119°$) and rectangular columnar phase ($a = 4.25$ nm, $b = 3.53$ nm)	3 transitions on the heating curve (17.6, 62.9, 82.1 °C) and 1 transition on the cooling curve (4.3 °C)	soft material	1 columnar phase ((40 °C heating): $a = 8.86$, $b = 5.63$ nm, $\gamma = 116°$) and 2 lamellar phases ((60 °C cooling): $d_0 = 3.61$, (72 °C heating) $d_0 = 3.57$ nm)

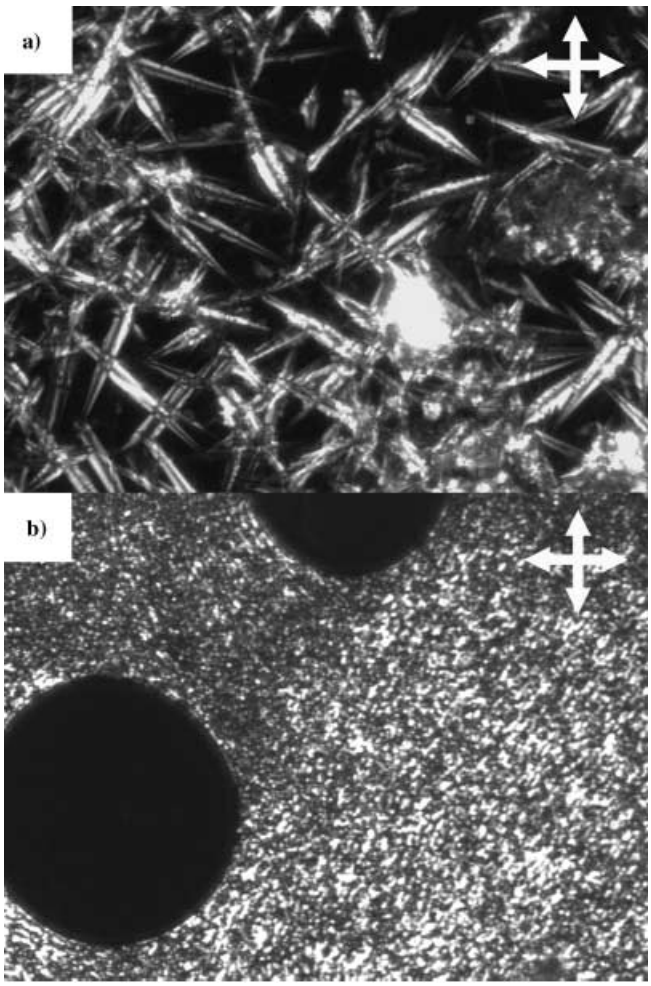

Figure 3. Copper–phenanthroline derivative–surfactant complexes viewed by optical microscopy under crossed polarizers: a) $CuCl_2$/BCS/C_{16}TAB complex at room temperature after heating at 160 °C; b) $CuCl_2$/BPS/DiC_{18}DAB complex at 90 °C after heating to 130 °C.

analyses showed no reflections in the wide-angle region, and only a broad reflection at approximately 20° (d spacing $\approx$0.45 nm) is found. This is indicative of a liquid-like arrangement of alkyl tails.

For the shorter-tailed DiC_{10}DA, DiC_{12}DA, and DiC_{14}DA surfactant complexes, the conformation of the central part of the complex induces unambiguous differences in the packing properties. In fact, with BPS, birefringent soft materials were obtained and a broad peak was detected in the SAXS patterns. This is in contrast to BCS complexes for which only isotropic, gel-like materials were obtained after casting from chloroform. With both chelating tectons, no transitions were observed in the DSC curves. It should be noted that the isotropic gels obtained with the complexes $[Cu^{I}(BCS)_2]\cdot(surfactant)_4$ can be aligned under shearing, and birefringence can be observed.

DiC_{16}DA complexes give a more optimized structure, as the alkyl subphase clearly is large enough to allow the formation of a new nanostructure. The material obtained with BPS is soft and birefringent (as before), showing no reflections in the wide-angle region. DSC measurements performed on this complex showed several thermal transitions on the first heating curve from room temperature to 150 °C, as often observed. It should also be noted here that the color of the film changes from green to black after the first heating curve; the absence of degradation was confirmed by TGA and IR analyses. A single broad and reversible transition centered at -19 °C is observed with an enthalpy of $\Delta H = 20.4\ J\,g^{-1}$ upon further thermal cycling studies. This broad transition is typical for structural rearrangements of the side chains, but presumably not related to major phase changes of the tectons. The SAXS pattern obtained directly after casting of the film show several peaks that cannot be indexed to a known phase and that are attributed to a kinetically frozen-in phase structure. Upon heating to 150 °C and subsequent re-cooling to room temperature, a marked decrease in the viscosity was noted, and a well-defined lamellar phase was observed with a lamellar repeat period of $d_0 = 3.95$ nm (Figure 4). The origin of the additional peak at 1.17 nm will be discussed later.

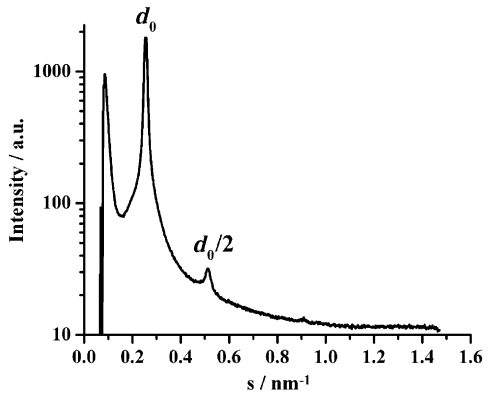

Figure 4. SAXS pattern of $CuCl_2$/BPS/DiC_{16}DAB complex at room temperature after heating to 150 °C (sample–detector distance = 40 cm).

No clear transitions were found after the first heating curve for the BCS complex with DiC_{16}DA; this material becomes liquid above 100 °C. After the samples had been allowed to cool back to room temperature, they retain their dark red color, and the absence of any color change was confirmed by solid-state UV/Vis measurements. Other than in the case of the shorter double-tail surfactants, the sample is now a noncrystalline, birefringent, soft material. The SAXS pattern obtained at room temperature, after the sample had been heated to 120 °C, also displays a broad peak ($d \approx 3.65$ nm), as in the case of DiC_{10}DA, DiC_{12}DA, and DiC_{14}DA complexes. Some additional peaks, indicative of higher order, were observed, but it was not possible to index these peaks to any known phase.

Following the trend of increasing complexity with increasing tail length of the double-tail surfactants, very highly organized materials were obtained for both ligands when they were complexed with double-tail C_{18} surfactants. Cu^{II}/BPS/DiC_{18}DA complexes displayed three transitions on the second heating curve (23.6, 63.9, and 113.1 °C) and two on the first cooling curve (102.7 and 11.1 °C) (Figure 5; arrows indicate the temperatures at which SAXS analyses were performed (as described below)). The structure of the complex as a function of temperature was monitored by SAXS. At room temper-

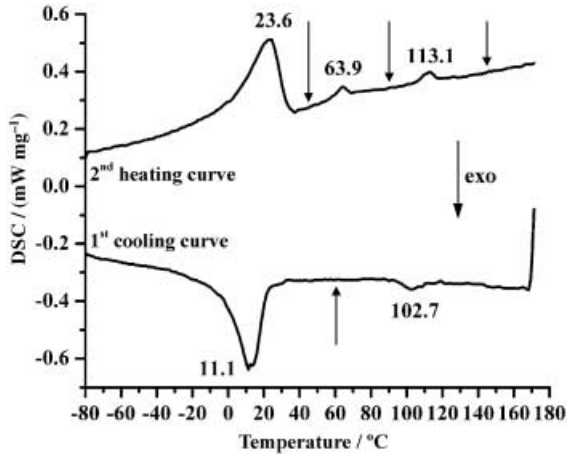

Figure 5. DSC curve of the complex $CuCl_2$/BPS/DiC_{18}DAB.

ature, a mixed phase is observed but no clear structure can be identified. At 145 °C, above the transition at 113.1 °C, the material is fluid and isotropic. At 60 °C, below the weak transition at 102.7 °C on the first cooling curve, the SAXS pattern displays a set of sharp peaks that can be indexed to an oblique columnar-phase system with the following crystallographic parameters: $a = 10.42$ nm, $b = 6.06$ nm, $\gamma = 123°$ (Figure 6).[21]

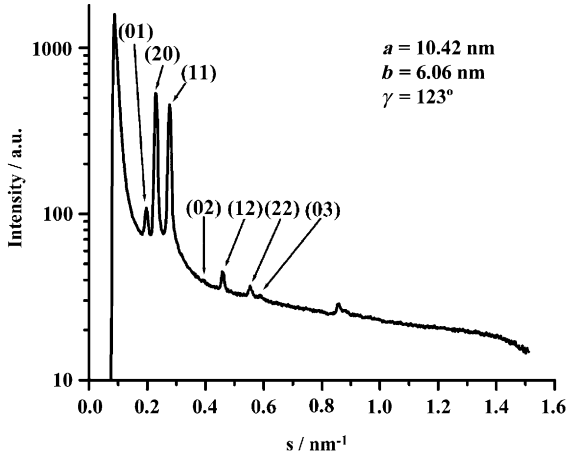

Figure 6. SAXS pattern of $CuCl_2$/BPS/DiC_{18}DAB complex at 60 °C after heating to 140 °C.

WAXS experiments performed at this temperature confirm the liquid-crystalline character of this material. The strong, reversible transition at low temperature (11.1 °C on the cooling curve) can be attributed to structural rearrangements of the side chains (crystallinity of the side chains confirmed by low-temperature WAXS measurements). In the second heating run between the transitions at 23.6 and 63.9 °C, a crystalline oblique columnar phase is observed at 45 °C, with parameters: $a = 10.06$ nm, $b = 5.86$ nm, $\gamma = 119°$. This oblique columnar phase changes to a liquid-crystalline rectangular columnar phase between 63.9 and 113.1 °C, with parameters of $a =$ 4.25 nm and $b = 3.53$ nm, as recorded at 90 °C.

A possible explanation for this behavior can be given: At low temperature a large unit cell is observed ($a = 10.06$ nm, $b = 5.86$ nm, $\gamma = 119°$), probably due to four different nonequivalent orientations of the columns within the material. At higher temperatures an increase in the thermal agitation renders the columns equivalent and consequently a smaller unit cell is obtained ($a = 4.25$ nm and $b = 3.53$ nm). Figure 7 shows the proposed model; the different shading indicates the different orientations of the tectonic units (alkyl tails not shown). An additional peak at 1.17 nm is observed in all the organized phases. The stacking distance of the complexes in the columns (forming both the oblique columnar phases and the lamellae, built-up by aligned columns) provides a possible explanation for the origin of this reflection. This fits with geometrical models of a tilted orientation of periodically organized phenanthroline units (size ca. 1.4 nm) around a Cu^{II} center.

Cu^{I}/BCS/DiC_{18}DA complexes also display several structural transitions. Three transitions can also be detected on the second heating curve (17.6, 62.9, 82.1 °C) but here only one clear transition can be observed on the first cooling curve (4.3 °C). This strong and reversible transition at low temperature (4.3 °C) must be attributed to structural rearrangements within the mesophases, as no crystallization of the side chains could be detected by WAXS. SAXS experiments also confirmed the presence of a mixed phase at room temperature after casting, and an isotropic state above the transition at 82.1 °C. However, despite the absence of visible transitions at high temperatures on the first cooling curve, a lamellar phase was detected in X-ray experiments at 60 °C, indicating an improvement of the structure and the existence of a real clearing point (but not on the time scale of DSC experiments). After the sample was cooled to −80 °C and then heated to 40 °C (on the second heating curve), sharp peaks were observed in the SAXS pattern. These are tentatively also indexed to an oblique columnar system ($a = 8.86$ nm, $b =$ 5.63 nm, $\gamma = 116°$). At 72 °C, a single lamellar phase with a lamellar repeat period of $d_0 = 3.57$ nm is observed. Here no

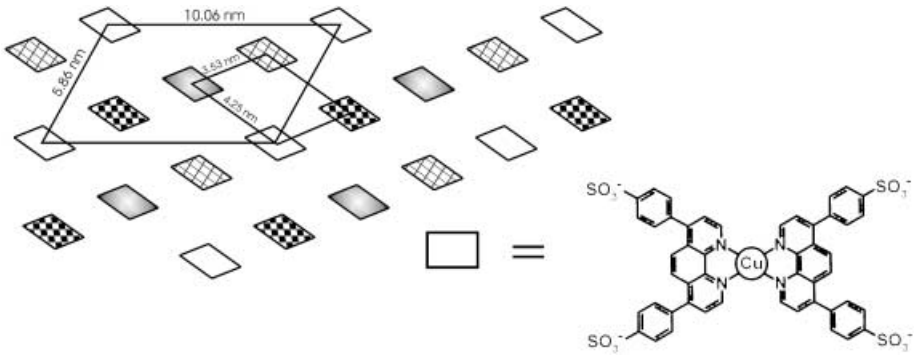

Figure 7. Model of the columnar phases of Cu^{II}/BPS/DiC_{18}DA obtained at 45 °C and 90 °C, showing the origin of the smaller unit cell at higher temperature (different shading indicates different orientation of the tectonic units, alkyl tails not shown).

peak indicative of an order inside the columns was detected, underlining that the tetragonal building block is less perfectly packed (higher symmetry) than the BPS structure.

Switchable materials properties: As mentioned before, all the green BPS complexes (in contrast to the red BCS complexes) turned black after they were heated to and kept at 150 °C for 4 h. No difference in behavior was observed regardless of whether the heating was carried out under vacuum or in air, which indicates that oxygen does not influence the process. No degradation of the BPS complexes took place, as revealed by TGA (less than 3% weight loss at 150 °C) and IR spectroscopy (no change of the recorded spectra). We therefore suggest that this color change must be due to a material-specific electronic transition. This specific electronic transition is evidenced by the appearance of a new absorption band in the UV/Vis spectra in the solid state and in solution at about 480 nm (Figure 8). No changes were observed in the rest of the UV spectra. This band is presumably related to the metal-to-ligand charge-transfer (MLCT) band at 479 nm observed for the BCS complexes with copper(I). The electronic transition is also evident from the absence of an EPR signal after the thermal treatment of the self-assembled film. This is indicative of a reduction of copper(II) to copper(I), or—less likely—the presence of antiferromagnetically coupled Cu^{II} ions. On the basis of experimental findings, we assign the transition to a change in the oxidation state of the copper ion inside the mesostructured film after heating. The exact origin of this electronic behavior is not clear since SAXS analyses did not show any significant structural changes before and after heating. Experiments are currently in progress to determine whether local changes around the metal center (such as the counterion species) influence this behavior.

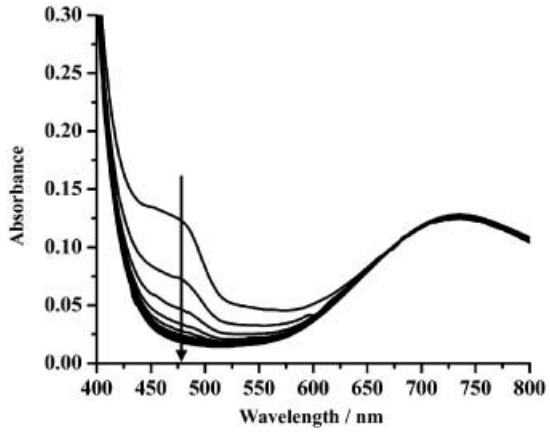

Figure 8. Time-dependent changes in the UV/Vis spectra of the black $CuCl_2$/BPS/DiC_{18}DAB redissolved in chloroform (1 min between each scan, $c = 2.6 \times 10^{-3}$ mol L^{-1}).

It should be noted that this change in oxidation state is reversible, since the resolubilisation of the film in chloroform leads to the formation of a green complex in solution (the original brown solution is transformed within minutes to a green solution). The UV/Vis spectra of such a redissolved film are comparable to that of the original complex (Figure 8). EPR measurements in solution also confirmed the reversible behavior, since a strong signal is obtained after several minutes. Films cast from these solutions exhibited the initial thermal behavior and phase structure.

Conclusion

We have demonstrated that a combination of ionic self-assembly (ISA) and classical metal coordination leads to the production of thermotropic liquid-crystalline materials. These metallomesogenic ISA materials, based on simple and accessible starting materials, exhibit typical phase morphologies such as lamellar and a variety of columnar phases. The phase behavior can easily be tuned by variation of the alkyl-tail volume fraction of the complexing surfactant species.

Besides these morphological aspects, an electromechanical switching process driven by the cooperative ISA process was also investigated. The oxidation state of the complexed metallic species (the central unit of the extended hybrid organic–inorganic tecton) was switched from Cu^{II} to Cu^{I}, which, through the results of a number of cross-experiments, was attributed to an improved packing behavior of the Cu^{I} species; that is, steric and cohesion energy effects entered the electrochemical potential of the central unit. A corresponding material-specific electronic transition was observed in the solid state as well. Through the application of a heating/dissolution cycle it was shown that this transition is reversible. Studies are currently in progress to determine the electronic properties of such switchable materials, because they might have potential for optical and electronic applications.

Finally, this work emphasizes the ability of ISA to be integrated within a stepwise noncovalent multiple-interaction cascade, and shows the potential of this method to access increased complexity and function of supramolecular materials.

Experimental Section

Ligands (BPS, bathophenanthrolinedisulfonic acid disodium salt ($C_{24}H_{14}N_2Na_2O_6S_2 \cdot 3H_2O$) and BCS, bathocuproinedisulfonic acid disodium salt ($C_{26}H_{18}N_2Na_2O_6S_2$)) were purchased from Merck and were used as received. Crystalline solid $CuCl_2 \cdot 2H_2O$ (99.999%) was purchased from Aldrich and used as received to prepare a light-blue stock solution (8 mmol L^{-1}) in deionized water. BPS (0.16 mmol, 94.5 mg; 2 equiv) or BCS (0.16 mmol, 90.3 mg; ; 2 equiv) dissolved in deionized water (10 mL) was added to the $CuCl_2$ solution (10 mL). The BPS and BCS solutions turned light green and olive green, respectively. These solutions were kept at room temperature under stirring for 24 h to ensure the coordination of the metallic center. Stoichiometric amounts (0.32 mmol, 4 equiv) of the cationic single- and double-tailed alkylammonium bromide surfactants (Aldrich, purity > 99%) dissolved in deionized water (10 mL) were added dropwise to the solutions of the copper–ligand complexes. Precipitation was observed after addition of the total amount of surfactant. The dispersions were kept under stirring for a further 24 h to ensure the complete exchange of the sodium ion by the alkylammonium surfactant. It should be noted that the BCS suspensions gradually turned from green to red on stirring at room temperature. This process was monitored by UV/Vis spectroscopy and, after 24 h, complete conversion of the complex was observed with a maximum of the absorption band at 479 nm. The precipitates were removed by centrifugation, washed twice with deionized water to remove the unbound counterions (NaBr), and dried under vacuum

(50 mbar) at room temperature. For the BPS ligand a green precipitate was obtained, whereas a deep red precipitate was obtained with the BCS ligand. In all the cases, except for the C_{10}TA complexes, these precipitates can be easily redissolved in chloroform, toluene, methanol, or acetone. After casting on Teflon-coated aluminum (BYTAC, Fisher) from chloroform, dark green or dark red films were obtained after evaporation of the solvent, depending on the original color of the complex. The films were dried under vacuum (50 mbar) at room temperature. EDAX and wide-angle X-ray scattering (WAXS) confirmed the removal of the sodium salts in these films. Elemental analysis (N, S) indicated that the 1:1 ratio of the complexation was fulfilled in the case of the double-tailed surfactants. Inductively coupled plasma optical emission spectrometry (ICP-OES) (Perkin Elmer Optima 3000) confirmed the stoichiometry of one copper atom for two phenanthroline molecules.

Elemental analyses were performed on a Vario EL Elementar (Elementar Analysen-systeme, Hanau, Germany). Differential scanning calorimetry (DSC) was performed on a Netzsch DSC 200. The samples were examined at a scanning rate of 10 K min^{-1} by applying two heating and one cooling cycle. Thermogravimetric analyses (TGA) were performed on a Netzsch TG 209. The samples were examined at a scanning rate of 20 K min^{-1} between room temperature and 300 °C.

Phase behavior was studied by polarized light optical microscopy (POM) on a Leica DM R microscope equipped with a Linkam TP92 heater with THMS 600 heating stage.

Small-angle X-ray scattering measurements were carried out with a Nonius rotating anode ($U = 40$ kV, $I = 100$ mA, $\lambda = 0.154$ nm) using image plates. With the image plates placed at a distance of 40 cm from the sample, a scattering vector range of $s = 0.07 - 1.6$ nm^{-1} was available. Two-dimensional (2D) diffraction patterns were transformed into 1D radial averages. The data noise was calculated according to Poisson statistics, which is a valid approach for scattering experiments. WAXS measurements were performed by using a Nonius PDS120 powder diffractometer in transmission geometry. A FR590 generator was used as the source of $Cu_{K\alpha}$ radiation ($\lambda = 0.154$ nm). Monochromatization of the primary beam was achieved by means of a curved Ge crystal. Scattered radiation was measured by using a Nonius CPS120 position-sensitive detector. The resolution of this detector in 2θ is 0.018°.

UV/Vis spectra were recorded by using a UVIKON 940/941 dual-beam grating spectrophotometer (Kontron Instruments) with a 1 cm quartz cell. UV/Vis solid-state measurements were performed on a Perkin – Elmer Lambda 2 spectrometer equipped with a Labsphere RSA-PE-20 Integration Sphere.

FT-IR spectra were collected by using an attenuated total reflectance (ATR diamond) accessory on a Fourier-transform BIORAD FTS 6000 spectrometer.

The electron paramagnetic resonance experiments were performed on solid samples and solutions ($CHCl_3$). The spectra were recorded in the X-band (= 9.5 GHz) on a Bruker ESP300E spectrometer at room temperature. The simulation of the spectrum was carried out with the program package WINEPR[22].

ICP-OES (Perkin Elmer Optima 3000) was used to determine the Cu content of the complexes. Each sample (20 mg) was first decomposed with HNO_3 (2 mL; 65 %) in a microwave (Anton Paar: Multiwave). The measurements of Cu were carried out at $\lambda = 324.75$ nm.

Acknowledgement

We thank the Max Planck Society and the Fund of the German Chemical Industry for financial support. Help with the X-ray measurements by Ingrid Zenke and technical help by Carmen Remde is gratefully acknowledged.

[1] a) J.-M. Lehn, *Angew. Chem.* **1990**, *102*, 1347 – 1362; *Angew. Chem. Int. Ed. Engl*, **1990**, *29*, 1304 – 1319; b) J.-M. Lehn, *Pure Appl. Chem.* **1994**, *66*, 1961 – 1966; c) J.-P. Sauvage, M. W. Hosseini in *Comprehensive Supramolecular Chemistry*, *Vol. 9* (Eds: J. L. Atwood, D. M. MacNicol, F. Vögtle, J.-M. Lehn), Elsevier, Oxford, **1996**; d) P. N. W. Baxter, J.-M. Lehn, B. O. Kneisel, G. Baum, D. Fenske, *Chem. Eur. J.* **1999**, *5*, 113 – 120; e) U. S. Schubert, C. Eschbaumer, *Angew. Chem.* **2002**, *114*, 3016 – 3050; *Angew. Chem. Int. Ed.* **2002**, *41*, 2892 – 2926.

[2] J. M. Lehn, *Supramolecular Chemistry: Concepts and Perspectives*, VCH, Weinheim, **1995**

[3] a) A. M. Giroud-Godquin, P. M. Maitlis, *Angew. Chem.* **1991**, *103*, 370; *Angew Chem. Int. Ed. Engl.* **1991**, *30*, 375 – 402; b) *Metallomesogens, Synthesis, Properties and applications* (Ed.: J. L. Serrano), VCH, Weinheim, **1996**; c) D. W. Bruce in *Inorganic Materials*, 2nd ed. (Eds.: D. W. Bruce, D. O′Hare), Wiley, Chichester, **1996**, Chapter 8, p. 429; d) B. Donnio, D. W. Bruce, *Struct. Bond.* **1999**, *95*, 193.

[4] a) J. Barbera, A. M. Levelut, M. Marcos, P. Romero, J. L. Serrano, *Liq. Cryst.* **1991**, *10*, 119 – 126; b) K. Binnemans, K. Lodewyckx, B. Donnio, D. Guillon, *Chem. Eur. J.* **2002**, *8*, 1101 – 1105.

[5] a) S. Munoz, G. W. Gokel, *J. Am. Chem. Soc.* **1993**, *115*, 4899 – 4900; b) S. J. P. Bousquet, D. W. Bruce, *J. Mater. Chem.* **2001**, *7*, 1769 – 1771; c) G. Pickaert, L. Douce, R. Ziessel, D. Guillon, *Chem. Commun.* **2002**, 1584 – 1585.

[6] Mudasir, M. Arai, N. Yoshioka, H. Inoue, *J. Chromatogr. A* **1998**, *799*, 171 – 176.

[7] Mudasir, N. Yoshioka, H. Inoue, *Talanta* **1997**, *44*, 1195 – 1202.

[8] a) A. Mohinfru, J. M. Fisher, M. Rabinovitz, *Nature* **1983**, *303*, 64 – 65; b) D. R. McMillin, K. M. McNett, *Chem. Rev.* **1998**, *98*, 1201 – 1219; c) D. A. Davis, A. A. Branca, A. J. Pallenberg, T. M. Marschner, L. M. Patt, L. G. Chatlynne, R. W. Humphrey, R. Yarchoan, R. L. Levine, *Arch. Biochem. Biophys.* **1995**, *322*, 127 – 134; d) S. Sethuraman, M. Palaniandavar, *Inorg. Chem.* **1998**, *37*, 693 – 700; e) D. S. Sigman, A. Mazumder, D. M. Perrin, *Chem. Rev.* **1993**, *93*, 2295 – 2316.

[9] D. Tran, B. W. Skelton, A. H. White, L. E. Laverman, P.C Ford, *Inorg. Chem.* **1998**, *37*, 2505 – 2511.

[10] F. Camerel, M. Antonietti, C. F. J. Faul, *Chem. Eur. J.* **2003**, 9, 2160 – 2166.

[11] a) C. F. J. Faul, M. Antonietti, *Chem. Eur. J.* **2002**, *8*, 2764 – 2768; b) Y. Guan, M. Antonietti, C. F. J. Faul, *Langmuir* **2002**, *18*, 5939 – 5945; c) Y. Guan, Y. Zakrevskyy, J. Stumpe, M. Antonietti, C. F. J. Faul, *Chem. Commun.* **2003**, 894 – 895.

[12] S. Chandrasekhar, B. K. Sadashiva, K. A. Suresh, *Pramana* **1977**, *9*, 471 – 480.

[13] a) H. C. Lip, R. A. Plowman, *Aust. J. Chem.* **1975**, *28*, 779 – 792; b) B. R. James, R. J. P. J. Williams, *J. Chem. Soc.* **1961**, 2007 – 2019; c) D. Blair, H. Diehl, *Talanta* **1961**, *7*, 163 – 174; d) A. E. Allan, A. G. Lappin, M. C. M. Laranjeira, *Inorg. Chem.* **1984**, 23, 477.

[14] a) F. S. Stephens, P. A. Tucker, J. Chem. Soc, *Dalton trans.* **1973**, 2293 – 2297; b) D. V. Scaltrito, D. W. Thompson, J. A. O′Callaghan, G. J. Meyer, *Coord. Chem. Rev.* **2000**, *208*, 243 – 266.

[15] M. K. Eggleston, D. R. McMillin, K. S. Koenig, A. J. Pallenberg, *Inorg. Chem.* **1997**, *36*, 172 – 176.

[16] F. K. Klemens, P. E. Fanwick, J. K. Bibler, D. R. McMillin, *Inorg. Chem.* **1989**, *28*, 3076 – 3079.

[17] A. A. Schilt, *Analytical Applications of 1,10-phenanthroline and related compounds*, Pergamon, New York, **1969**.

[18] Mudasir, M. Arai, N. Yoshioka, H. Inoue, *J. Chromatogr. A* **1998**, *799*, 171 – 176.

[19] a) A. M. Dittler-Klingemann, C. Orvig, E. F. Hahn, F. Thaler, C. D. Hubbard, C. van Eldik, S. Shindler, I. Fabian, *Inorg. Chem.* **1996**, *35*, 7793 – 7803; b) G. De Santis, L. Fabbrizzi, D. Lacopino, P. Pallavicini, A. Perotti, A. Poggi, *Inorg. Chem.* **1997**, *36*, 827 – 832.

[20] R. Ziessel, L. Chardonnière, M. Cesario, T. Prangé, H. Nierengarten, *Angew. Chem.* **2002**, 114, 1017 – 1021; *Angew. Chem. Int. Ed.* **2002**, *41*, 975 – 979.

[21] a) M. L. Bushey, A. Hwang, P. W. Stephens, C. Nuckolls, *J. Am. Chem. Soc.* **2001**, *123*, 8157 – 8158; b) A. F. Thünemann, D. Ruppelt, C. Burger, K Müllen, *J. Mater. Chem.* **2000**, *10*, 1325 – 1329.

[22] R. T. Weber, *Win-EPR-Symfonia Version 1.2*, EPR Division, *Bruker Instruments Inc.* **1995**.

Received: December 20, 2002
Revised: March 4, 2003 [F4693]

